Computers in Biology and Medicine 78 (2016) 97–106

Contents lists available at ScienceDirect

Computers in Biology and Medicine

journal homepage: www.elsevier.com/locate/cbm

Extraction and processing of videocapsule data to detect and measure the presence of villous atrophy in celiac disease patients

Edward J. Ciaccio [a,*], Govind Bhagat [a,b], Suzanne K. Lewis [a], Peter H. Green [a]

[a] Celiac Disease Center, Department of Medicine, Columbia University Medical Center, New York, United States
[b] Department of Pathology and Cell Biology, Columbia University Medical Center, New York, United States

ARTICLE INFO

Article history:
Received 8 July 2016
Received in revised form
5 September 2016
Accepted 14 September 2016

Keywords:
Celiac disease
Images
Small intestine
Tutorial
Videocapsule
Villous atrophy

ABSTRACT

Background: Videocapsule endoscopy is a relative new method to analyze the gastrointestinal tract for the presence of pathologic features. It is of relevance to detect villous atrophy in the small bowel, which is a defining symptom of celiac disease.
Method: In this tutorial, methods to extract and process videocapsule endoscopy data are elucidated. The algorithms, computer code, and paradigms to analyze image series are described in detail. The topics covered include extraction of data, analysis of texture, eigenanalysis, spectral analysis, three-dimensional projection, and estimation of motility. The basic paradigms to implement these processes are provided.
Results: Examples of successful quantitative analysis implementations for selected untreated celiac disease patients with villous atrophy versus control patients with normal villi were illustrated. Based on the implementations, it was evident that celiac patients tended to have a rougher small intestinal texture as compared with control patients. From three-dimensional projection, celiac patients exhibited larger surface protrusions emanating from the small intestinal mucosa, which may represent clumps of atrophied villi. The periodicity of small intestinal contractions tends to be slower when villous atrophy is present, and the estimated degree of motility is reduced as compared with control image series. Basis image construction suggested that fissuring and mottling of the mucosal surface is predominant in untreated celiac patients, and mostly absent in controls.
Conclusions: Implementation of computerized methods, as described in this tutorial, will likely be useful for the automated detection and measurement of villous atrophy, and to map its extent along the small intestine of celiac patients.

1. Introduction

Celiac disease is a major health issue in many parts of the world, but it is unknown to many and often remains undiagnosed [1]. Yet, left untreated, the disease can cause many harmful effects, including damage to the nervous system and cancer [2]. The disease is caused by reactivity to gluten, a protein found in wheat, rye, and barley grains, and similar protein components [3]. There is only one effective treatment thus far developed – abstinence from consuming gluten and its components. Yet, most persons do not maintain the diet unless diagnosed as having the disease. Diagnosis of celiac disease is difficult owing to the presence of occult symptoms [4]. A defining manifestation is the presence of villous atrophy in the small intestine, which can be detected in biopsy specimens acquired during standard endoscopy using light microscopy. However, the presence of villous atrophy in the small intestinal mucosa is often patchy and subtle [5]. It is not so readily evident by visual observation based on the endoscopic imaging technology that is readily available at the present time. Thus, the need for a computerized means for detection of villous atrophy.

If villous atrophy could be detected based on computerized analysis of endoscopic images, it would go a long way toward improving success in diagnosing the disease in many more patients. Yet, with standard endoscopy, distal regions of the small intestine, in the jejunum and ileum, where villous atrophy is sometimes present, cannot be analyzed due to the limited locational ability of the technique. More recently, videocapsule endoscopy has been introduced to enable the observation of the entire small intestine for presence of pathologic features [6–8]. Videocapsule endoscopy consists of a small swallowable capsule with camera and light source that acquires high-resolution images from the small intestine at periodic intervals. The imaging data is transferred via radio link to a receiver console for subsequent analysis. Although the videocapsule images are currently acquired at a rate of approximately 2 frames per second and a resolution of

* Correspondence to: HP 934, Columbia University, 180 Fort Washington Avenue New York, NY 10032, United States.
E-mail address: ejc6@columbia.edu (E.J. Ciaccio).

http://dx.doi.org/10.1016/j.compbiomed.2016.09.009
0010-4825/

576 × 576 pixels, this temporal and spatial resolution is not wholly adequate to observationally determine the structure of the small intestinal villi and their status as being either normal or atrophied. If computerized methods could be implemented for quantitative analysis, it would be useful for improved efficacy to detect and measure the presence of villous atrophy all along the small intestinal tract [7]. Such information might possibly reduce the need for standard endoscopy and intestinal biopsy, thus decreasing invasiveness, and likely decreasing procedural cost as well.

In prior work, the extraction and quantification of videocapsule endoscopy data was studied for the analysis of untreated celiac patients with villous atrophy versus control patients with normal villi [7,9–13]. The purpose of this tutorial is to show methods of implementation in terms of the algorithms, flow of computer code, and paradigms for successful analysis. Herein, techniques that have been noted to be useful for detection of villous atrophy in celiac disease patients will be defined and described in detail, so that they can be readily implemented on any computer system for analysis of videocapsule data.

2. Method

In this section, the clinical methods, the videocapsule device specifications, the implementation of algorithms for videocapsule data analysis, and the presentation of relevant paradigms for computer code will be described and discussed. Implementation of the computer code provided enables the rapid analysis of data on PC-type computers.

2.1. Clinical methods

Retrospective use of videocapsule endoscopic data was approved by the Internal Review Board of Columbia University Medical Center. Adult patients that were referred for videocapsule analysis included both confirmed celiac disease patients and controls. Only in the celiac patients was villous atrophy present in the small intestinal mucosa. Based on a prior analysis of small intestinal biopsies obtained by standard endoscopy and imaged under light microscopy, the severity of villous atrophy in the celiac patients ranged from Marsh Score II–IIIc. Control patients with either obscure bleeding or suspected Crohn's disease were used for quantitative comparison. Both male and female patients were included for analysis.

2.2. Description of the videocapsule

The videocapsule device used for imaging was the Pillcam SB2 (Given Imaging, Ltd, Yoqneam, Israel). The plastic capsule size is 11 × 26 mm, the weight is 2.8 g, the videocamera field of view is 156°, and it acquires 2 images per second [14]. The battery life is 8 h, with an image resolution of 576 × 576 pixels. The capsule is disposable. It consists of an imaging device, a compact lens, a white light emitting diode which acts to illuminate the gastrointestinal mucosa, and an internal battery. The entire wireless capsule system consists of a videocapsule endoscope, a sensing and recording system which is attached via a belt to the patient, and a computer console with proprietary software (RAPID v6.5, Given Imaging). After fast, the patient swallows the capsule with water, and can then undergo normal daily activity. Data transmission is via ultra-high frequency radio band telemetry. Once the data stream is downloaded, representative images and videoclips can be annotated and stored to PC hard drive or removable media. Contraindications for this procedure include known or suspected gastrointestinal obstruction, presence of a cardiac pacemaker or implantable cardioverter defibrillator, swallowing disorder, and pregnancy of the female patient.

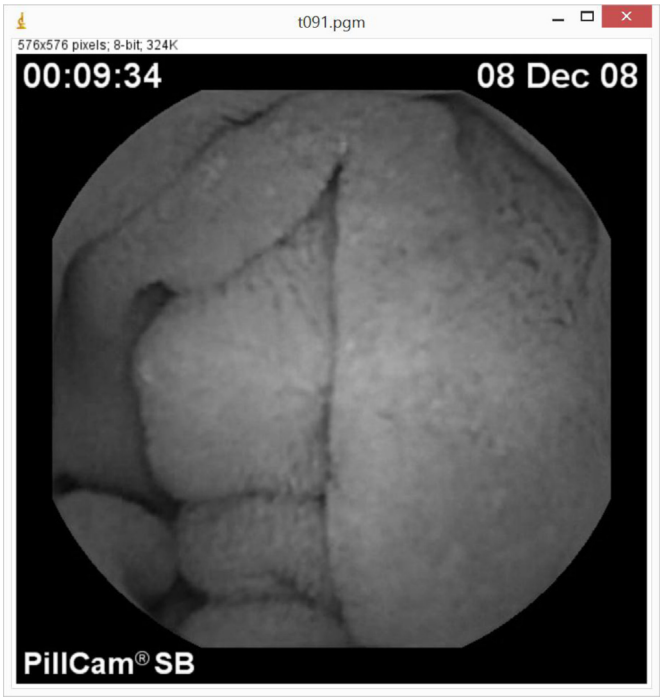

Fig. 1. Celiac disease endoscopic image used to show data format in the PGM file.

2.3. PGM image format specification

Once the imaging data is downloaded, although videocapsule images are initially stored as tricolor data, for simplicity, reduced storage requirement, and ease of use, the information is first transformed to grayscale level. The Portable Gray Map specification (PGM or pgm) is a straightforward method for encoding grayscale images that is used for this purpose. The format of PGM images is comprised of several components, which are described in detail in the Appendix, Part A. The graylevel is embedded in the file data for a total of 576 × 576 pixels, and therefore 576 × 576 grayscale values, i.e., 331,776 pixels in all. In Fig. 1, this data is displayed using the ImageJ program [15]. Depicted is an image of the small intestinal mucosa from a control patient. At the top left of the image, the ImageJ program displays the spatial resolution (576 × 576 pixels), grayscale level (8 bit or 256 levels), and the rounded total number of pixels contained in the image. Additional information that is embedded in the image is also shown – the date that the image was acquired, patient code, and imaging model (Pillcam SB). The borders are black by default in the Pillcam system. The image itself only consists of the portion within the black borders. ImageJ, as a program that can display PGM images, provides the information about the image resolution at top and displays with white borders.

2.4. Extraction of imaging data

To obtain PGM images for analysis, the computer program in the Appendix, Section B, can be used. The program plays a color mpeg videoclip, and then stores the individual frames as 256-level grayscale PGM images in ASCII. The reading of videoclips that are made in other formats, and the writing of the separate images to other formats or to a binary file, can be readily done by changing a few of the parameters. The play speed for the movie, 2 per second for the Given Imaging system application, can be altered via the last parameter in the movie function, and can be used to slow

down or speed up play. The code was implemented in MATLAB ver. 7.7.0, R2008b (The MathWorks, Natick, MA). Only the main MATLAB program, not any of the toolboxes, is required for it to run.

In the first portion of the program, the number of image frames is automatically determined, and the video frames are prepared to play successively in color (Appendix, Part A). In the second portion of the program, the movie is played, with the frame rate given as 2 per second, which is the same as the record speed. To slow the movie down, this number could be decreased to 1 per second, and to speed it up, it would be increased. The movie frames are also converted to grayscale and then written to disk as PGM images. The image is saved to folder C:/folder/im in this example.

Based on this paradigm, PGM images can be readily acquired from an MPEG movie clip obtained during videocapsule endoscopy. Once the PGM graylevel images are stored to disk, it is straightforward to prepare them for processing. The pixel level grayvalues are provided as a sequential set of numbers which is composed of 331,776 elements. These elements are ordered row by row, 576 elements per row, and 576 rows, from left to right and top to bottom, with only space delimiters separating each pixel graylevel value and no extra delimiters used to denote the end of a row. This data can then be rapidly read into other computer programs for further processing.

2.5. Three-dimensional projection and syntactic analysis

A first step in the analysis of the data is to display the structural components contained in the two-dimensional image by projecting it to three dimensions. A useful algorithm to do this is shown in the Appendix, part C. The code first initializes parameters (lines 1 and 2). The user is then asked for the file number to process (line 3). The file is opened, the first line is read, and the data is input all at once as a vector p of length 331,776. The file is then closed, and the counter n is initialized to a value of 0 (line 4). The information is then read and arranged from vector p to a matrix m of size 576×576 (lines 5–7). Two files are opened, one to display the brightness level (line 9) and the other to display locational information (line 10). Then in lines 11–19, a moving average filter with 11×11 kernel size is implemented to smooth the data. The display of the three-dimensional data is done using the map3d program [16]. The .pot file, used by map3d, provides grayscale level only, which can be assessed to generate a false-color three-dimensional image. The .pts file, also used by map3d, provides the three-dimensional data in Cartesian coordinates, where the first two dimensions are the X and Y axis locations of the pixel, and the third dimension (Z-axis) is the smoothed grayscale level.

The transformation process from graylevel to Z-axis position is based on the principles of shape-from-shading. In prior work, it has been shown that the transformation of two-dimensional endoscopic images to three-dimensional projections is useful to detect endoscopic image structure that would not readily be detectable by visual inspection [9,10]. Thus, using this projection, it would be possible to determine whether features unique to areas with villous atrophy were present in the data. An example of the process is shown in Fig. 2. In panel A is provided an image acquired by videocapsule endoscopy. In panel B is its three-dimensional counterpart. The image has been rendered as a three-dimensional volume. False color can be added (panel C) to further accentuate the volume rendering. The top series is from a celiac patient while the lower series is from a control patient. The structure of the celiac patient information can be quite readily observed in the three-dimensional images, with the presence of large protrusions or nodules, which are particularly evident in the false color image at right, as compared with the false color image for the control patient. It has been shown that in areas with villous atrophy, the size of the mucosal nodules, some of which are noted by asterisks in the images, are enlarged as compared with control subjects [9,10].

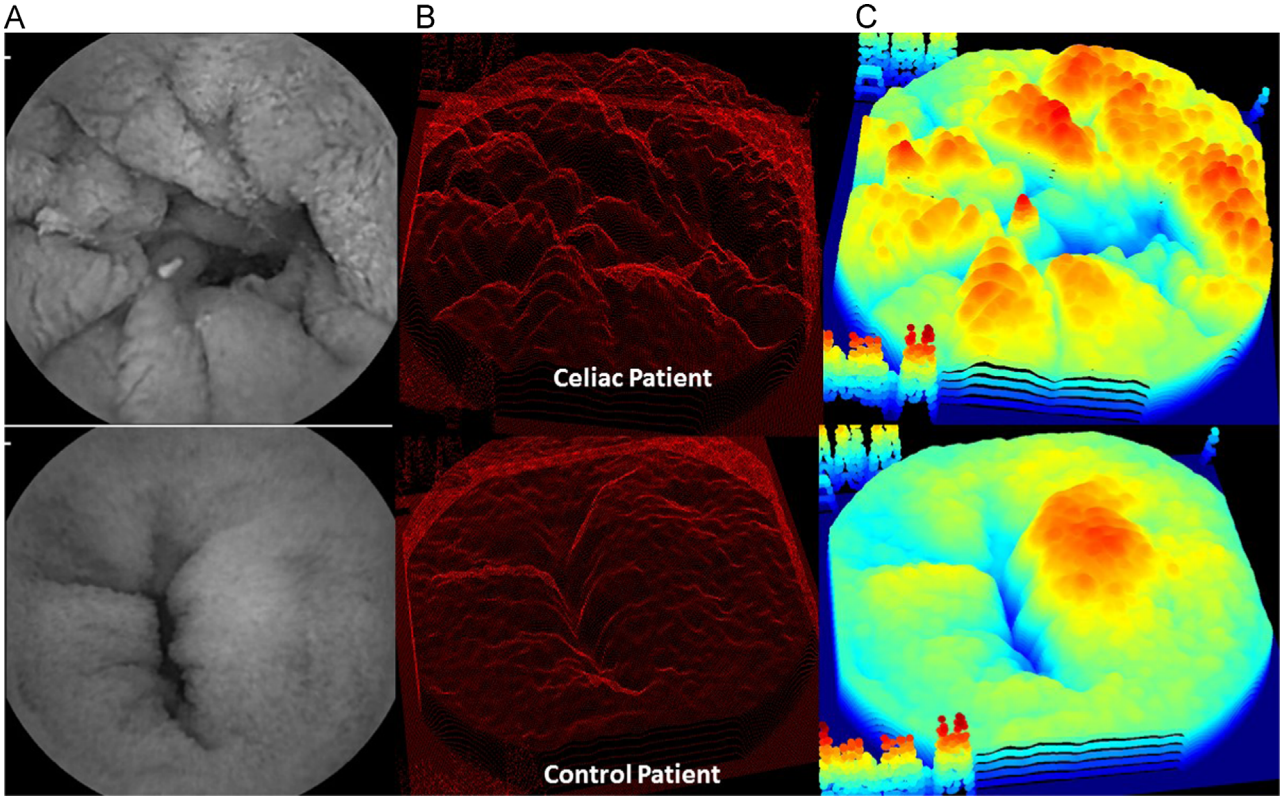

Fig. 2. Examples of original two-dimensional endoscopic images (A), three-dimensional projection images (B), and false color three-dimensional projections (C). (For interpretation of the references to color in this figure legend, the reader is referred to the web version of this article.)

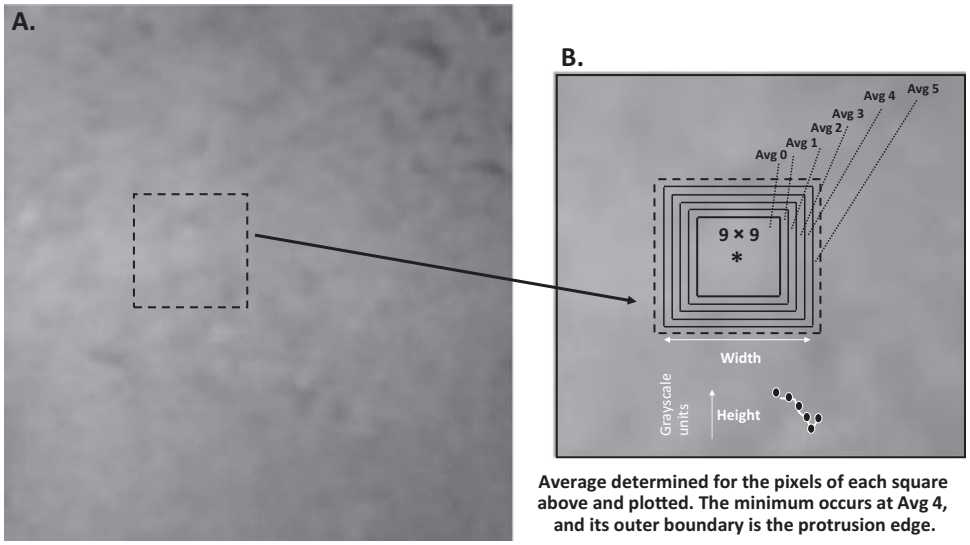

Fig. 3. Syntax for a mucosal protrusion is shown. The syntax is used to detect and estimate the geometry of all mucosal protrusions for all images in the videoclip series.

Mucosal protrusions, as are evident in Fig. 2, can be automatically detected using a specialized syntax [7,9]. The syntax used as a first step to model the protrusion was based on a square geometric figure. A summary diagram is shown in Fig. 3. At left, a larger area of image is shown. The dashed black square in the image represents a bright area which is at the center of a mucosal protrusion. The area searched by the algorithm is shown at right in Fig. 3. The average graylevel of each concentric square is determined. The outer edge of the protrusion is defined as that concentric square in which the average graylevel no longer diminishes as compared with the adjacent inner square. This is illustrated in the graph below the image. From this outermost, concentric square component, the dimensions of the protrusion are estimated. The width and length of the protrusion are defined as the width and length of the concentric square in pixels. The height of the protrusion is defined as the difference in average graylevel from the outer concentric square to the innermost concentric square. This process is repeated for all bright areas in the image. Therefore, the dimensions of all protrusions, and the number of such protrusions per image, can be recorded. The paradigm for detecting mucosal protrusions and for measuring their geometry is as follows.

1. Smooth the entire image data (11×11 kernel is typically used).
2. Use another kernel to detect protrusions. The kernel consists of a pixel region, square in shape.
3. If the pixel with maximum brightness is at the center of the kernel, a peak is detected.
4. If a peak is detected, determine the average pixel brightness for center and for concentric rings outward from the bright central pixel.
5. The edge of the protrusion coincides with the last outer ring in which grayscale level decreases.
6. Since a square model is used, the estimated protrusion length and width have the same value.
7. The protrusion height is the difference in average grayscale level between center and outer edge.
8. The protrusion volume would be the product of length $\times$ width $\times$ height.

Once a protrusion is detected, its height, width, length, area, and volume are calculated and tabulated.

2.6. Motility estimation

Although actual gastrointestinal motility can be measured with strain gauge devices or with a three-dimensional imaging system, indirect methods exist to assess motility of the gastrointestinal tract from two-dimensional endoscopic image series. In Fig. 4 are shown examples of a motility estimating system [17]. The luminal center is anticipated to be, as a first approximation, the region with darkest pixels in the image, since darker areas are likely to be furthest from the camera light source. At left are unretouched images from an untreated celiac disease patient. At right are the corresponding images with the darkest 10,000 pixels highlighted. Coordinate data for the retouched images are provided at right. The centroid of the darkest pixels region (x,y) is taken as the actual center. The maximum width w is also shown, which is delineated as a red bar in the image. The standard deviation of the (x,y) center can be calculated over the entire image series. The obtained parameters can be used as a rough estimate of gastrointestinal motility, and correspond to the movement of the lumen center with respect to the changing camera angle of the videocapsule. Although the size of the luminal center varies, for simplicity, the region encompassed by the darkest 10,000 pixels out of the total number of pixels in each image ($576 \times 576 = 331776$) was considered to be the luminal center. The paradigm for detecting the luminal center is as follows.

1. Determine the location of the darkest 10,000 image pixels of 331,776 total.
2. Calculate the centroid of this region, which may not be continuous.
3. The x value of the centroid is the average x location for all 10,000 darkest pixels.
4. The y value of the centroid is the average y location for all 10,000 darkest pixels.
5. Determine the maximum contiguous width of the 10,000 darkest pixels as an additional measure.
6. Over the image series, calculate the standard deviation in these parameters as a measure of motility.

Another indirect measure of motility can be obtained be estimating the periodicity of endoscopic image features [18]. As a rough approximation, the mean graylevel of each image can be utilized to determine the periodicity. This is illustrated in Fig. 5. At top are a series of endoscopic images of differing grayscale level,

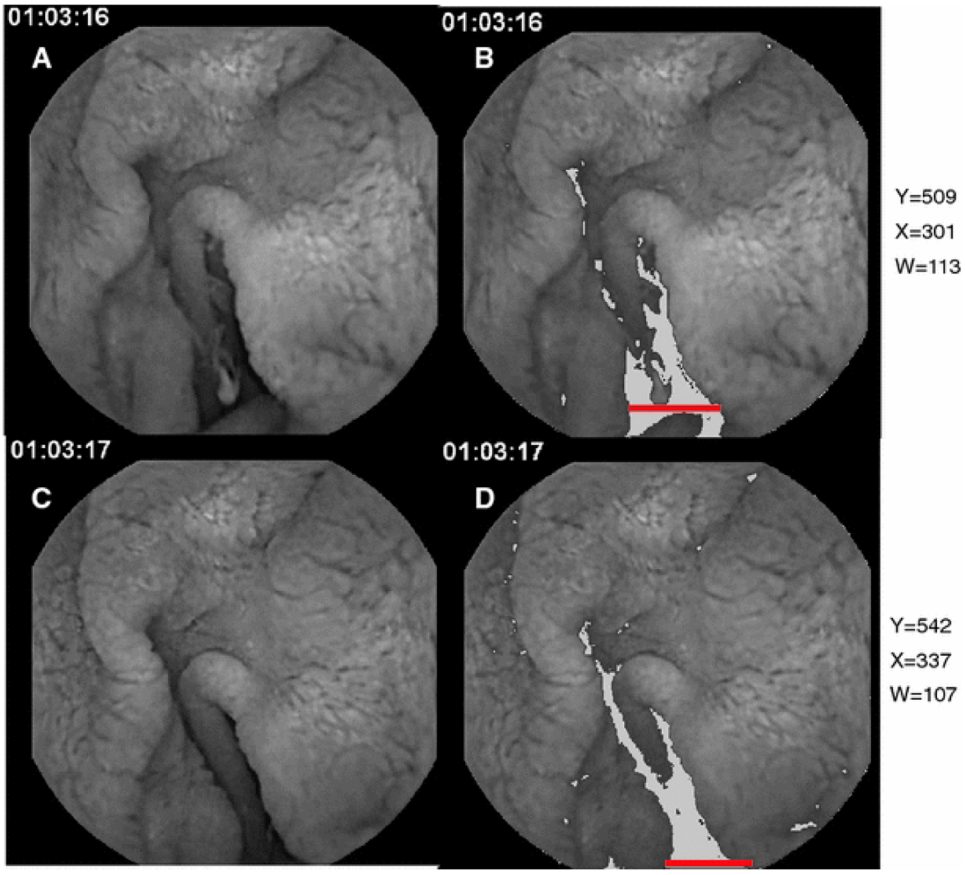

Fig. 4. Example of the central lumen calculation. The darkest 10,000 pixels are an estimate of central lumen location, as highlighted in the corresponding images at right. (For interpretation of the references to color in this figure, the reader is referred to the web version of this article.)

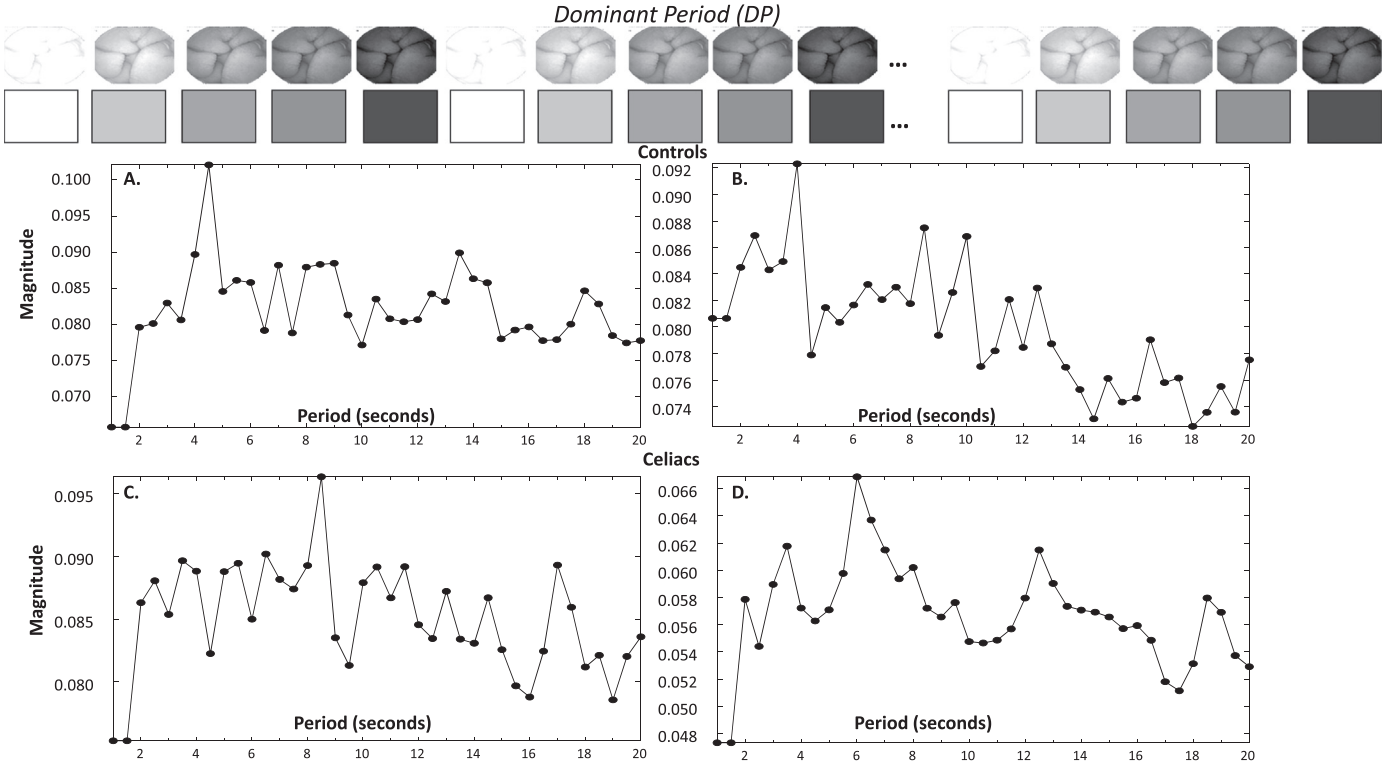

Fig. 5. Schematic of the dominant period (top) and spectra from actual control (A-B) and celiac patient (C-D) videoclip data. The period of untreated celiac patient components tends to be longer than for controls.

which was artificially created for illustration purposes. The graylevel goes from white to dark gray and back again over three periods. The average graylevel is shown beneath each endoscopic image. For this series, the period of the largest component is 5 image frames, or 2.5 s, for the frame rate of 2 per second. Therefore 2.5 s is the dominant period for this synthetic image series. In panels A–D of Fig. 5, spectra from actual celiac versus control image series are shown. The control spectra are displayed at top (A and B) and the celiac spectra in the lower panels (C and D). Note that the dominant period for the control image spectra, which is the highest peak in each spectrum, have lower values (i.e., shorter time periods) as compared with the untreated celiac patient spectra. The control patient dominant periods are approximately 4 s in length, which correspond to a frequency of approximately 0.25 Hz. In contrast, the celiac spectra have dominant periods of approximately 7–8 s, corresponding to frequencies of approximately 0.125 Hz. Thus the periodicity of celiac image series features is much longer, about twice as long, as the control patient series in this example. Software used to estimate the periodic components of a videoclip image series is described as follows.

1. Determine the average graylevel in each image.
2. Create a time series from the average graylevel for all images.
3. Compute the power spectrum. This is done by -

   a. segment the time series into n segments of length:

   $\ell =$ int(N/n), where $N=$ the number of images (200).
   b. Compute ensemble average vector ℓ for each set of segments of length ℓ.
   c. Compute the root mean square (RMS) power for each ensemble average vector ℓ.
   d. Plot the power spectrum as RMS power of ℓ versus segment length (period) ℓ.
4. The largest nonharmonic peak in the spectrum is the dominant period DP.
5. Based on the likely gastrointestinal periodicity, the spectral range is generally 3–40 image time epochs, i.e., 1.5–20 s at 2/s frame rate.

2.7. Construction of basis images

Salient image features can be obtained via a transformation [12,19]. Rather than estimating the syntax from a single image, the entire videoclip series of images is used for this purpose in order to accentuate salient features that are present repetitively in the image series. The images are summed based on periodicity. Features that appear during those time epochs will be reinforced in the ensemble average (i.e., basis image). A similar calculation is done for other periods, so that basis images can be obtained at all frequencies of interest. Examples of basis images are shown in Fig. 6 for control (top) and celiac patient data (lower). Note that the control basis images appear smoother, with less varied features. In contrast, the celiac images contain a higher degree of heterogeneity. There are evident curved lines representing recurring fissuring, as well as very light and very dark areas, giving a mottled appearance in the celiac basis images. The more textured celiac basis images are likely due to the presence of standout pathologic structures in the image series. Construction of basis images from a videoclip series is detailed in the following paradigm.

1. From the power spectrum, determine the periodicity to use to generate basis images. Using the dominant period or DP will likely reveal a rich set of features because it is the largest periodic component.
2. Suppose for example, that the DP is 10 time epochs (=10 image frames or 5 s), then:
   a. Sum images 1, 11, 21, 31, … 191 and divide by 20 to form an ensemble average.
   b. Sum images 2, 12, 22, 32, … 192 and divide by 20 to form an ensemble average.
   c. Sum images 3, 13, 23, 33, … 193 and divide by 20 to form an ensemble average.
   d. … sum images 10, 20, 30, 40, … 200 and divide by 20 to form an ensemble average.
3. There are therefore 10 basis images that can be formed for period 10. These basis images will contain salient features having a periodicity of 10 image frames.
4. The 10 basis images for period 10 show features that appear at different time lags.

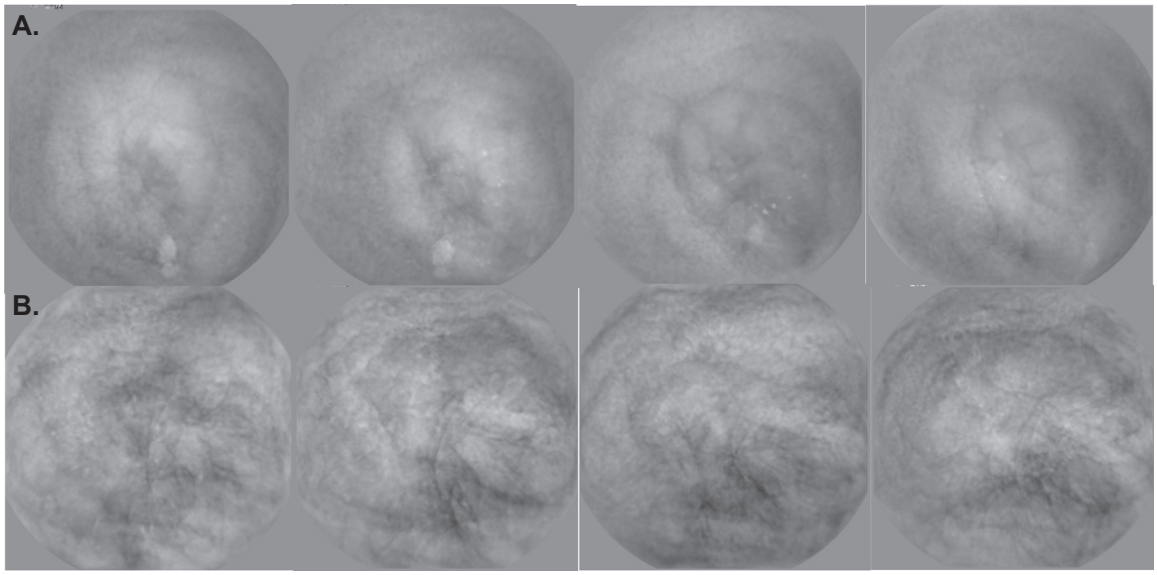

Fig. 6. Examples of basis images for a control patient (top) and for an untreated celiac patient (lower). Many rougher salient features are evident in the celiac patient data.

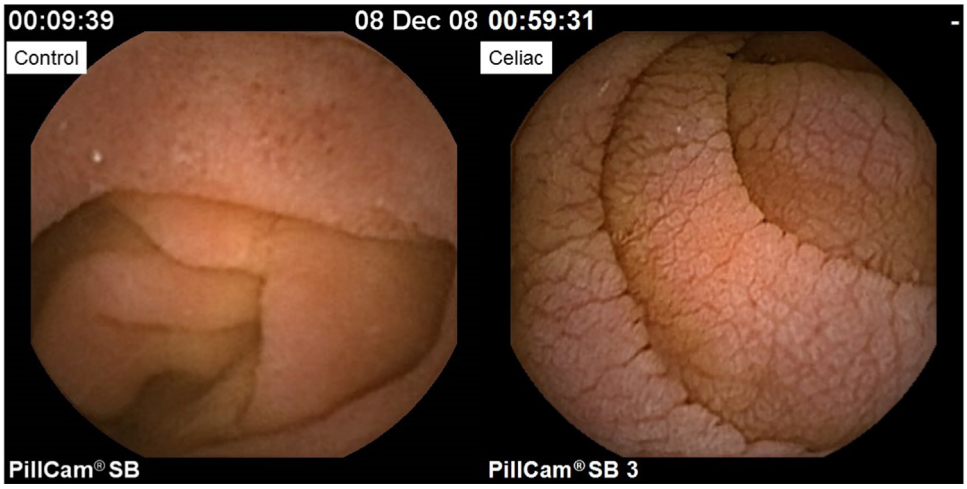

Fig. 7. Examples of full color videocapsule endoscopic images for control patient (left) and celiac patient (right). The celiac patient image, acquired with the PillCam SB 3 system, has a much rougher apparent texture. (For interpretation of the references to color in this figure legend, the reader is referred to the web version of this article.)

2.8. Textural components

Textural properties are also important to quantitatively compare celiac versus control images, and for characterizing the presence of villous atrophy [20]. In Fig. 7, color videocapsule images from a control patient (left) and from a celiac patient (right) are shown. The control patient image contains mostly homogeneous mucosal surfaces. Smooth edges of the mucosal folds are also evident. In contrast, the mucosal surface in the celiac patient image has a much rougher evident texture. A large magnitude of fissuring is present, as is scalloping of the mucosal folds. There is a slightly mottled appearance of the mucosal surface throughout the image. A guide for extraction of texture (first and second central statistical moments), and the use of 10×10 pixular subimages to estimate spatial variability, shown in Fig. 8, are provided in the paradigm below.

1. Calculate the mean (brightness level) and standard deviation (variation) in pixel graylevel for each 10×10 subimage.
2. There are $576/10 \times 576/10$ subimages per image $=56 \times 56=3136$ per image.
3. Determine the average for the brightness level and variation for all subimages in the image.
4. Calculate the mean and standard deviation in brightness level and variation from the averages for all images in the series.

3. Discussion

3.1. Summary

To the present time, less quantitative research is being done on celiac disease topics as compared to the amount of biomedical research being done, for example, on food allergies [21,22]. Herein, a number of methods, algorithms, paradigms, and computer code details useful for extracting and analyzing videocapsule endoscopy data were presented and described in detail. The presented methods have been shown in past studies to be efficacious for distinguishing videocapsule images series of celiac disease patients with villous atrophy, versus control patient data exhibiting normal small intestine villi [10]. Firstly, the need for computerized methods of image extraction from capsule videoclips was considered, and a technique to do so via MATLAB coding was presented. The method extracts grayscale PGM images from the videoclips, with PGM being selected due to its readily interpretable format for encoding image data. The PGM images are stored separately to computer disk, and are available for visual inspection via the ImageJ program [15]. ImageJ can even be used for further quantitative analysis of these images, although to do so is not discussed herein.

Once the grayscale images are separately stored as individual files, they are ready for processing. A shape-from-shading

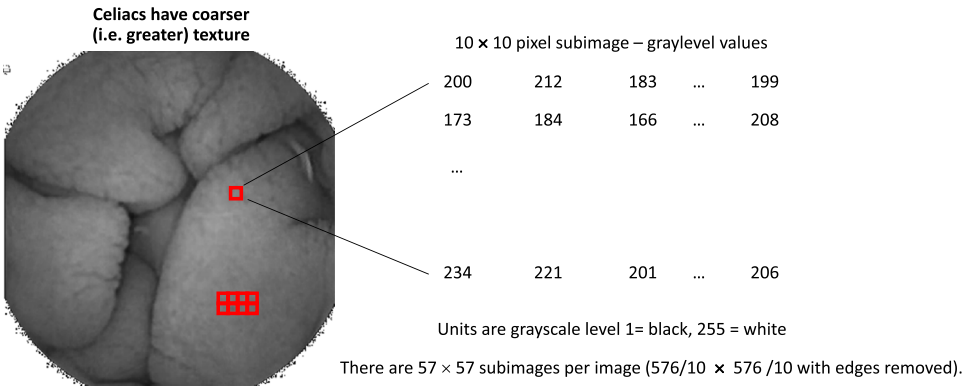

Fig. 8. Extraction of texture from an endoscopic image. The mean (first statistical moment) and standard deviation (second central moment) are calculated. 10×10 subimages are used to show the spatial variation in texture.

technique has been introduced to transform the two-dimensional grayscale endoscopic images into three-dimensional projection images [9,10]. The third axis, or Z-axis, i.e. depth, was calculated directly from the graylevel values of the original image. The three-dimensional projection images are of potential utility to provide an estimate of the actual topography of the small intestinal mucosa. In contrast, the topography of the small intestinal mucosa is not as readily evident in two-dimensional images for analysis, either by computerized means or by direct visual inspection. An example of three-dimensional topography, and the presence of possibly pathologic features, was shown in Fig. 2, which included enlarged surface protrusions, that may represent clumps of atrophied villi, and surface fissuring, in an untreated celiac patient. The three-dimensional structural information was used to build a syntax for describing the mucosal surface protrusions. As a first approximation, surface protrusions can be modeled as a simple geometric shape such as a circular or square object [9,10]. For simplicity in the paradigm outlined in this study, a square ring model was chosen to represent the structure of the protrusions. These features are then detected when the average pixular grayscale level of concentric square rings progressively diminishes outward from the bright center. The length, width, and height of each protrusion are automatically measured based on the boundary point of outermost ring contained in the protrusion. Examples were given, and in prior work it was shown that in untreated celiac patients, these protrusions are significantly larger in dimension as compared to those present in control patients lacking villous atrophy [9,10].

An indirect measure of gastrointestinal motility was then presented [17]. The motility of the small intestinal wall was approximated by the variation in location of the distal luminal cavity. This area was modeled as a very dark grayscale level of pixels. The centroid of this region, which is the mean location along the X and Y axes, was considered to be the direction of the distal lumen. Due to motion, the Cartesian coordinates (x,y) of this location changed over the image series, and therefore over time. In prior work, it was found that motility as measured via this metric is less in untreated celiac patients as compared with controls with normal villi [17]. Another indirect means of measuring small intestinal motility that was introduced was to calculate the dominant period [18]. Although as a first approximation, average grayscale level throughout each image, plotted for all successive images in the videoclip series, was used as a measure of periodicity, more sophisticated algorithms might possibly be developed to determine the periodic components in the image series. The dominant period was defined as the most predominant periodic component in the frequency spectrum of the image series. The dominant period has been found to be longer in untreated celiac patients as compared with control patients having normal villi [18]. The longer periodic nature of the untreated celiac data suggests that the peristaltic waves, an indicator of motility, are slower and longer between contractions, at least at areas with villous atrophy in the celiac patients.

As a measure of the salient features present in the small intestinal mucosa, basis images can be obtained from each videoclip [12,19]. These transform images are calculated using an ensemble averaging technique that considers feature periodicity. It was found in prior work that the celiac patient basis images contain many more abnormal structural features including the presence of dark curved lines and patchy areas with differing grayscale level, as compared with controls [12]. The dark curved lines likely represent the fissuring which is commonly present at the macroscopic level in celiac patients with significant villous atrophy, while dark patches may represent areas with a greater degree of villous atrophy, giving rise to the mottled pattern often evident in celiac patient endoscopic images. Basis images are a composite of the features that periodically appear in some images in the series, and therefore they represent predominant features that recur. In celiacs, there are a number of such abnormal-looking features throughout each basis image, while in control patients, many of the basis images are quite uniform and homogeneous in appearance, thus likely representing smooth and normal villi throughout the small intestine. The differing basis images at a particular periodicity represent the differing feature content appearing at phase lags.

A more ubiquitous metric for discerning image content is the texture, and textural parameters were also introduced in the methods provided [6,20]. In order to account for spatial as well as temporal differences in texture, each 576×576 pixel image was subdivided into 10×10 subimages throughout. The texture in each of these subimages was separately calculated, and statistical moments were determined to compare and contrast the degree of texture and the variability in texture between celiac patients and controls. It has been shown that celiacs tend to have rougher texture, perhaps owing to the fact that there are macroscopic pathologic structures commonly present in areas with villous atrophy [9,10]. These structures typically are composed of varying texture and often, as in the presence of fissuring and mottled appearance, a darker grayscale level, and a more varied grayscale level over the entire image (spatial domain), and from image to image (time domain). This gives rise to both the rougher texture and to the larger variation in texture measured in the celiac patient images. Although the videocapsule resolution in both spatial and temporal domains is still quite limited, it is possible, with improved resolution, to further resolve types of texture and distinct textural components in the endoscopic images. This could be assistive to determine where precisely actual villous atrophy resides, for improved localization to biopsy, as well as to distinguish degrees of villous atrophy based on the different characteristics of the textural features.

3.2. Clinical perspective

Videocapsule endoscopy is a relatively new technique with the potential to revolutionize the analysis of the small intestinal mucosa for evidence of pathology [23]. If the presence and degree of villous atrophy could be determined based on videocapsule imaging, it would eliminate the need for the more invasive method of standard endoscopy to be used. It could also eliminate the need for determining locations where villous atrophy, which is patchy, may reside as a target for biopsy in those areas. The lack of finding of a suitable area to biopsy the small intestine when villous atrophy is actually present would mean that the patient would likely be misdiagnosed as not having the disease, and / or would require repeat procedures when it is still suspected. Although it is not currently feasible to obtain a biopsy using videocapsule endoscopy, this is likely to be possible in future manifestations of the capsule due to advances in the technology, and could be used, for example, as a confirmatory procedure once actual areas with suspected villous atrophy were identified by computerized analysis of the image sequence [23]. Since the method is computerized, and the algorithms carry very little computational cost, results would be available in real time and therefore could also be used to guide any future biopsy device that might be available within the capsule. Even at present, the computerized methods described herein can be useful for identifying likely regions of villous atrophy retrospectively, and to gauge the degree of villous atrophy in each patient.

It is important to determine the magnitude of any villous atrophy in addition to its presence and location, so as to monitor the health of celiac disease patients [24]. Although a gluten-free diet is important for restoring the health of the small intestinal

villi in celiac patients, as well as to restore the normal function elsewhere in the body when affected by the autoimmune reaction, it requires monitoring for several reasons [25]. Firstly, food labeled as gluten-free may not actually be entirely gluten-free due to cross-contamination [25]. Moreover, the patient may make mistakes and accidentally, or even intentionally, ingest gluten-containing foods. Furthermore, it is possible that the patient may have refractory disease and not respond well to a gluten-free diet, in which case villous atrophy and other systemic symptoms of the disease will likely remain. All of these circumstances require careful monitoring of the progress of recovery, or lack thereof, in the small intestinal villi. By automating and computerizing the process of videocapsule endoscopy analysis, observer bias is eliminated, subtle pathology can be detected, and there is the possibility to map the entire small intestine, not only the proximal portion as with standard endoscopic means [10].

3.3. Other quantitative methods useful to detect abnormality

A number of other quantitative methods, some of which are quite sophisticated for quantitative analysis, have been developed and found useful to detect abnormalities in endoscopic images acquired from celiac patients. The use of local texture operators has been shown to achieve the best overall accuracy of the various feature extraction techniques to detect duodenal texture patches with pathology (two class problem) [26]. The use of spatio-temporal features and automated systems are also promising concepts in videocapsule endoscopy analysis [27]. A syntactic technique has been developed which included the use of shape-based features to describe local curvature along the edges of image components, and is helpful for classification [28]. A major image representation method that has been devised involves the use of an Edge Co-occurrence Matrix, which embeds information about the edges of image components within the matrix [27]. Wavelet-based methods are also commonly applied for endoscopic image analysis of the small intestinal mucosa to detect pathology [27]. Additionally, scale-invariant features have been applied to enable robust analysis when camera perspectives (angle and rotation) and distances vary in the endoscopic sequences [29].

3.4. Limitations and future directions

In the study a number of methods were presented to quantitatively analyze the small intestinal mucosa in untreated celiac patients versus controls. These methods can be implemented in software code, and are likely to be portable to most computers and operating systems. However, as individual computer characteristics vary, it might be necessary to alter the code slightly in order to fit the specific parameters of the computer system at hand. Provided herein were several methods for detecting the presence of villous atrophy. It is likely that these methods will be useful adjuncts when comparing and contrasting patients with suspected or confirmed villous atrophy, and to monitor the alterations which occur over time, owing to the fact that the basic characteristics that can be extracted from the videoclip image series were considered – the motility estimates, textural operators, three-dimensional structural characteristics and the resulting syntax that can be developed, as well as the repetition of abnormal features evident in the basis images. The code presented does not represent a complete, automated and turnkey system. That is left for future, more commercially oriented designs, which might be helpful in improving future imaging systems for videocapsule analysis of celiac disease. Comparison of results before and after treatment can also provide important information and should be done in future studies.

Conflicts of interest

No.

Appendix

Part A: portable gray map (PGM) specification

The PGM image file is composed of the following components –.

1. An alphanumeric number which identifies the file type. For PGM, the encoded number is 'P2'.
2. The encoded number is followed by whitespace (space, tab, carriage return, and / or line feed).
3. The image width in number of pixels, formatted as decimal ASCII characters.
4. Whitespace.
5. The image height in number of pixels, formatted as decimal ASCII characters.
6. Whitespace.
7. The maximum graylevel value, formatted as decimal ASCII characters.
8. Single whitespace character.
9. The image data with graylevel values.

The image data appears in the image from top left to bottom right (raster scan mode).

Part B. Video image extraction

The following program can be used in MATLAB to display an endoscopic videoclip as a movie on the computer screen, and to extract and write to disk PGM images from the videoclip.

```
% Construct an object associated with the mpeg videoclip.
readerobj=mmreader('C: /folder/filename.mpg', 'tag',
  'myreader1');
% Read in all video frames and obtain the number of frames.
vidFrames=read(readerobj);
numFrames=get(readerobj, 'numberOfFrames');
% Create a MATLAB movie structure from the video frames.
for k=1: numFrames
    mov(k).cdata=vidFrames(:,:,:,k);
    mov(k).colormap=[ ];
end

% Create figure, resize from video dimensions, playback at
  frame rate (2/s).
hf=figure;
set(hf, 'position', [150 150 readerobj. Width readerobj. Height]);
movie(hf, mov, 1, 2);
% Write movie frames to individual grayscale files (pgm
  format).
for k=1: numFrames
    imwrite(mov(k).cdata, ['C: /folder/im' num2str(k, '%.3d') '.
  pgm'], 'pgm', 'Encoding', 'ASCII');
end
```

Part C. Three-dimensional volume rendering

To obtain a three-dimensional projection of the two-dimensional image data, the following computer code can be utilized. This is an example of a complete, turnkey program:

```
ccccccccccc initialize variables ccccccccccc
      integer m(576,576), p(331776)
      character g*8, y*35, f*3
      print*, 'file #'; read(5,*) f
ccccccccccc read in parameters and data ccccccccccc
      open(8, file='t'//f//'.pgm'); read(8,*) y(1:2); read(8,*) p; close(8); n=0
      do 8 l=1, 331776-576, 576
          n=n+1
          m(n,1:575)=p(l:l+575)
8     continue
ccccccccccc prepare files to write to for map3d ccccccccccc
      open(8, file='p'//f(1:3)//'hh2.pot')
      open(9, file='t'//f(1:3)//'hh1.pts')
ccccccccccc smooth grayscale data, 11 x 11 kernel ccccccccccc
      do 19x=6, 570, 2
      do 19y=6, 570, 2
          z=0.
          do 17 k=-5, 5
          do 17 j=-5, 5
              z=z+float(m(x+k, y+j))/121.
17        continue
cccc write coordinate information, z (depth) is the mean graylevel cccc
          write(8,*) z; write(9,*) x, y, z
19    continue
20    stop; end
```

References

[1] P.H. Green, B. Jabri, Coeliac disease, Lancet 362 (2003) 383–391.
[2] P.H. Green, A.T. Fleischauer, G. Bhagat, R. Goyal, B. Jabri, A.I. Neugut, Risk of malignancy in patients with celiac disease, Am. J. Med. 115 (2003) 191–195.
[3] A. Fasano, I. Berti, T. Gerarduzzi, T. Not, R.B. Colletti, S. Drago, Y. Elitsur, P. H. Green, S. Guandalini, I.D. Hill, M. Pietzak, A. Ventura, M. Thorpe, D. Kryszak, F. Fornaroli, S.S. Wasserman, J.A. Murray, K. Horvath, Prevalence of celiac disease in at-risk and not-at-risk groups in the United States: a large multicenter study, Arch. Intern. Med. 163 (2003) 286–292.
[4] W. Lo, K. Sano, B. Lebwohl, B. Diamond, P.H. Green, Changing presentation of adult celiac disease, Dig. Dis. Sci. 48 (2003) 395–398.
[5] V.H. Shah, H. Rotterdam, D.P. Kotler, A. Fasano, P.H. Green, All that scallops is not celiac disease, Gastrointest. Endosc. 51 (2000) 717–720.
[6] E.J. Ciaccio, C.A. Tennyson, S.K. Lewis, S. Krishnareddy, G. Bhagat, P.H. Green, Distinguishing patients with celiac disease by quantitative analysis of videocapsule endoscopy images, Comput. Methods Progr. Biomed. 100 (2010) 39–48.
[7] E.J. Ciaccio, G. Bhagat, S.K. Lewis, P.H. Green, Suggestions for automatic quantitation of endoscopic image analysis to improve detection of small intestinal pathology in celiac disease patients, Comput. Biol. Med. 65 (2015) 364–368.
[8] T. Rokkas, Y. Niv, The role of video capsule endoscopy in the diagnosis of celiac disease: a meta-analysis, Eur. J. Gastroenterol. Hepatol. 24 (2012) 303–308.
[9] E.J. Ciaccio, C.A. Tennyson, G. Bhagat, S.K. Lewis, P.H. Green, Use of shape-from-shading to estimate three-dimensional architecture in the small intestinal lumen of celiac and control patients, Comput. Methods Progr. Biomed. 111 (2013) 676–684.
[10] E.J. Ciaccio, C.A. Tennyson, G. Bhagat, S.K. Lewis, P.H. Green, Implementation of a polling protocol for predicting celiac disease in videocapsule analysis, World J. Gastrointest. Endosc. 5 (2013) 313–322.
[11] E.J. Ciaccio, C.A. Tennyson, G. Bhagat, S.K. Lewis, pH. Green, Methods to quantitate videocapsule endoscopy images in celiac disease, Biomed. Mater. Eng. 24 (2014) 1895–1911.
[12] E.J. Ciaccio, C.A. Tennyson, G. Bhagat, S.K. Lewis, pH. Green, Use of basis images for detection and classification of celiac disease, Biomed. Mater. Eng. 24 (2014) 1913–1923.
[13] E.J. Ciaccio, G. Bhagat, S.K. Lewis, pH. Green, Quantitative image analysis of celiac disease, World J. Gastroenterol. 21 (2015) 2577–2581.
[14] ASGE Technology Committee, Wireless capsule endoscopy: technology status evaluation report, Gastrointest. Endosc. 78 (2013) 805–815.
[15] C.A. Schneider, W.S. Rasband, K.W. Eliceiri, NIH Image to ImageJ: 25 years of image analysis, Nat. Methods 9 (2012) 671–675.
[16] map3d: Interactive scientific visualization tool for bioengineering data, Scientific Computing and Imaging Institute (SCI), Downloaded from: ⟨http://www.sci.utah.edu/cibc/software.html⟩.
[17] E.J. Ciaccio, C.A. Tennyson, G. Bhagat, S.K. Lewis, P.H. Green, Quantitative estimates of motility from videocapsule endoscopy are useful to discern celiac patients from controls, Dig. Dis. Sci. 57 (2012) 2936–2943.
[18] E.J. Ciaccio, C.A. Tennyson, G. Bhagat, S.K. Lewis, P.H. Green, Robust spectral analysis of videocapsule images acquired from celiac disease patients, Biomed. Eng. Online 10 (2011) 78.
[19] E.J. Ciaccio, C.A. Tennyson, G. Bhagat, S.K. Lewis, P.H. Green, Transformation of videocapsule images to detect small bowel mucosal differences in celiac versus control patients, Comput. Methods Progr. Biomed. 108 (2012) 28–37.
[20] E.J. Ciaccio, C.A. Tennyson, G. Bhagat, S.K. Lewis, P.H. Green, Classification of videocapsule endoscopy image patterns: comparative analysis between patients with celiac disease and normal individuals, Biomed. Eng. Online 9 (2010) 44.
[21] E.J. Ciaccio, G. Bhagat, S.K. Lewis, P.H. Green, Trends in celiac disease research, Comput. Biol. Med. 65 (2015) 369–378.
[22] E.J. Ciaccio, G. Bhagat, S.K. Lewis, P.H. Green, Trends in Gluten research and its relationship to autoimmune and allergic diseases, Informatics in Medicine Unlocked. 3 (2016) 7-17.
[23] P. Swain, The future of wireless capsule endoscopy, World J. Gastroenterol. 14 (2008) 4142–4145.
[24] P.H.R. Green, C. Cellier, Celiac disease, N. Engl. J. Med. 357 (2007) 1731–1743.
[25] A.R. Lee, D.L. Ng, E. Dave, E.J. Ciaccio, P.H. Green, The effect of substituting alternative grains in the diet on the nutritional profile of the gluten-free diet, J. Hum. Nutr. Diet. 22 (2009) 359–363.
[26] A. Vécsei, G. Amann, S. Hegenbart, M. Liedlgruber, A. Uhl, Automated Marsh-like classification of celiac disease in children using local texture operators, Comput. Biol. Med. 41 (2011) 313–325.
[27] S. Hegenbart, A. Uhl, A. Vécsei, Survey on computer aided decision support for diagnosis of celiac disease, Comput. Biol. Med. 65 (2015) 348–358.
[28] M. Gadermayr, M. Liedlgruber, A. Uhl, A. Vécsei, Evaluation of different distortion correction methods and interpolation techniques for an automated classification of celiac disease, Comput. Methods Progr. Biomed. 112 (2013) 694–712.
[29] S. Hegenbart, A. Uhl, A. Vécsei, G. Wimmer, Scale invariant texture descriptors for classifying celiac disease, Med. Image Anal. 17 (2013) 458–474.